Supplement of Hydrol. Earth Syst. Sci., 27, 1477–1492, 2023
https://doi.org/10.5194/hess-27-1477-2023-supplement

Hydrology and Earth System Sciences
Open Access
EGU

Supplement of

Hydrological response to climate change and human activities in the Three-River Source Region

Ting Su et al.

Correspondence to: Chiyuan Miao (miaocy@vip.sina.com)

Supplementary materials

Table S1. Characteristics of 13 runoff-related parameters tested for sensitivity analysis and model optimization.

Parameter	Brief description	Units	Range
B	Shape of the variable infiltration capacity curve controlling surface runoff	N/A	0.001–0.4 [a]
D_1	Thickness of upper soil layer	m	0.01–0.5 [b]
D_2	Thickness of middle soil layer	m	0.05–1.0 [a]
D_3	Thickness of bottom soil layer	m	0.5–2.5 [a]
D_s	Fraction of maximum velocity of baseflow	N/A	0.001–1 [a]
D_m	Maximum velocity of baseflow	mm/day	5–20 [a]
W_s	Fraction of maximum soil moisture content of bottom soil layer	N/A	0.1–1 [a]
E_1	Exponent of Brooks–Corey drainage equation for upper soil layer	N/A	8–30 [b]
E_2	Exponent of Brooks–Corey drainage equation for middle soil layer	N/A	8–30 [b]
E_3	Exponent of Brooks–Corey drainage equation for bottom soil layer	N/A	8–30 [b]
K_1	Saturated hydraulic conductivity in upper soil layer	mm/day	163–4765 [c]
K_2	Saturated hydraulic conductivity in middle soil layer	mm/day	163–4765 [c]
K_3	Saturated hydraulic conductivity in bottom soil layer	mm/day	163–4765 [c]

[a] Source: Shi et al. (2008). [b] Source: Demaria et al. (2007). [c] Source: Bennett et al. (2018).

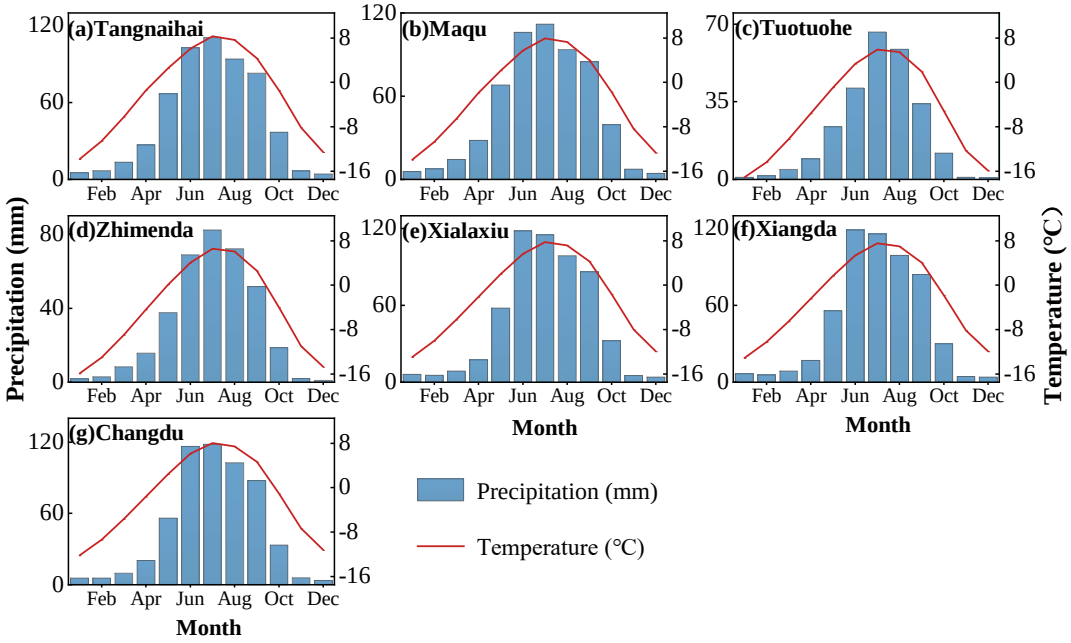

15 **Figure S1. Mean monthly precipitation and temperature for the seven stations (a–g) during 1984–2018.**

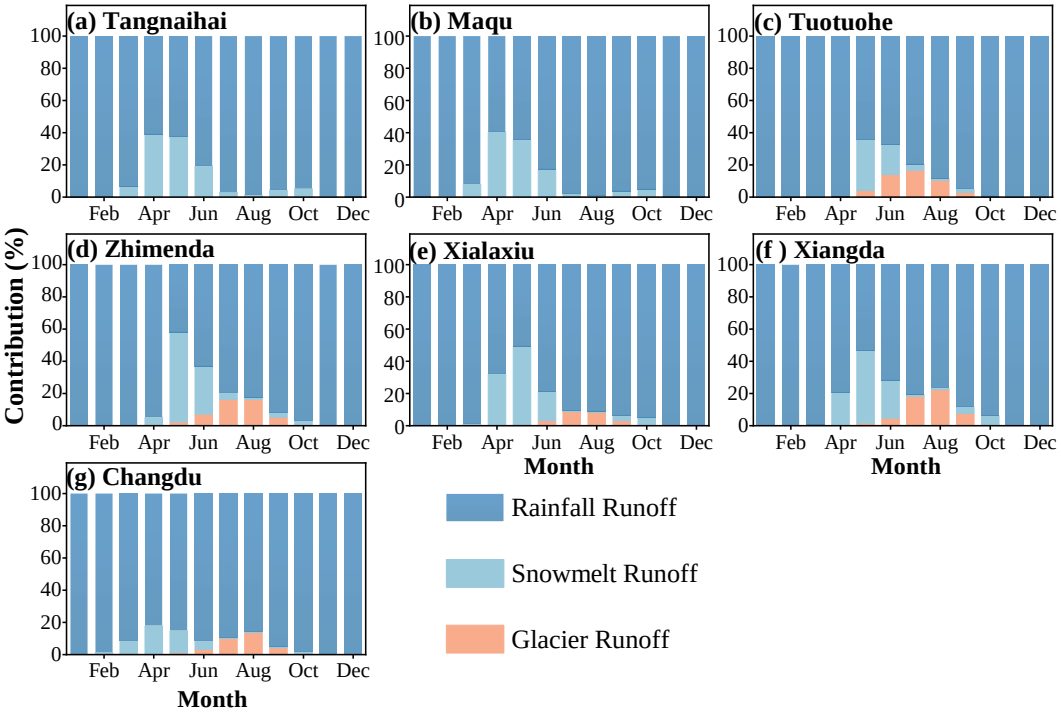

Figure S2. Contributions of rainfall, snowmelt, and glacier runoff to the total monthly runoff for the seven stations (a–g) during 1984–2018.

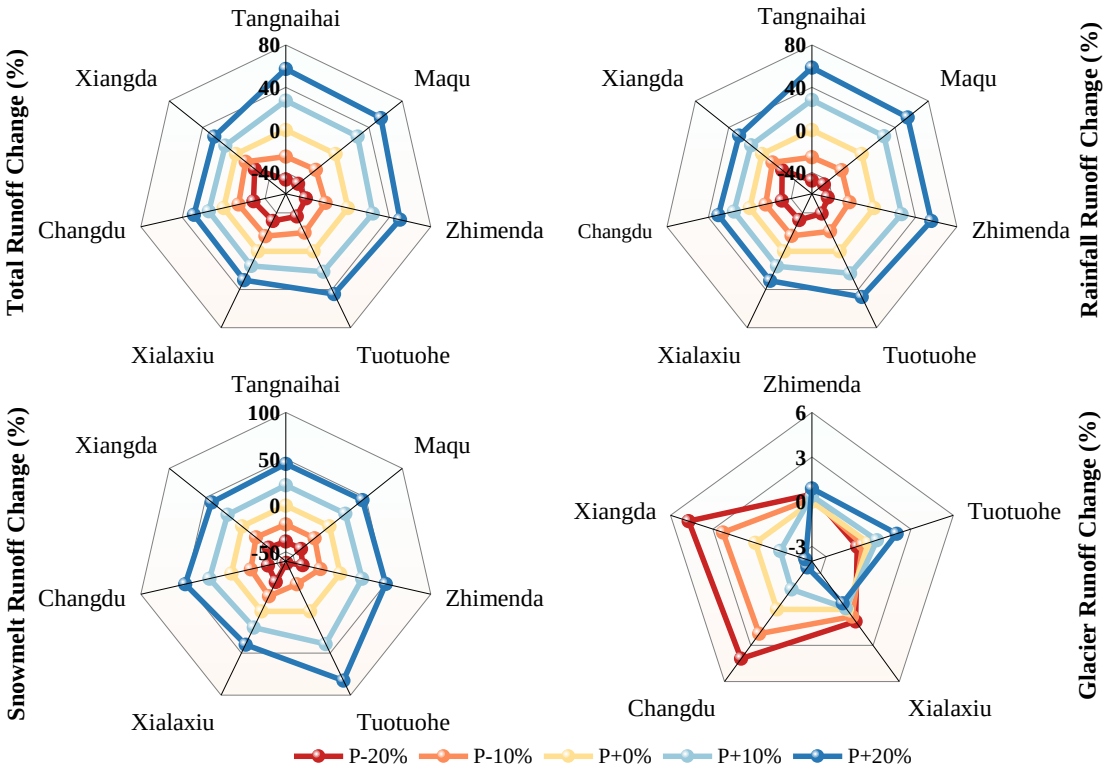

Figure S3. Percentage change in mean annual total, rainfall, snowmelt, and glacier runoff relative to the period 1984–2018 under precipitation-change scenarios for the seven stations.

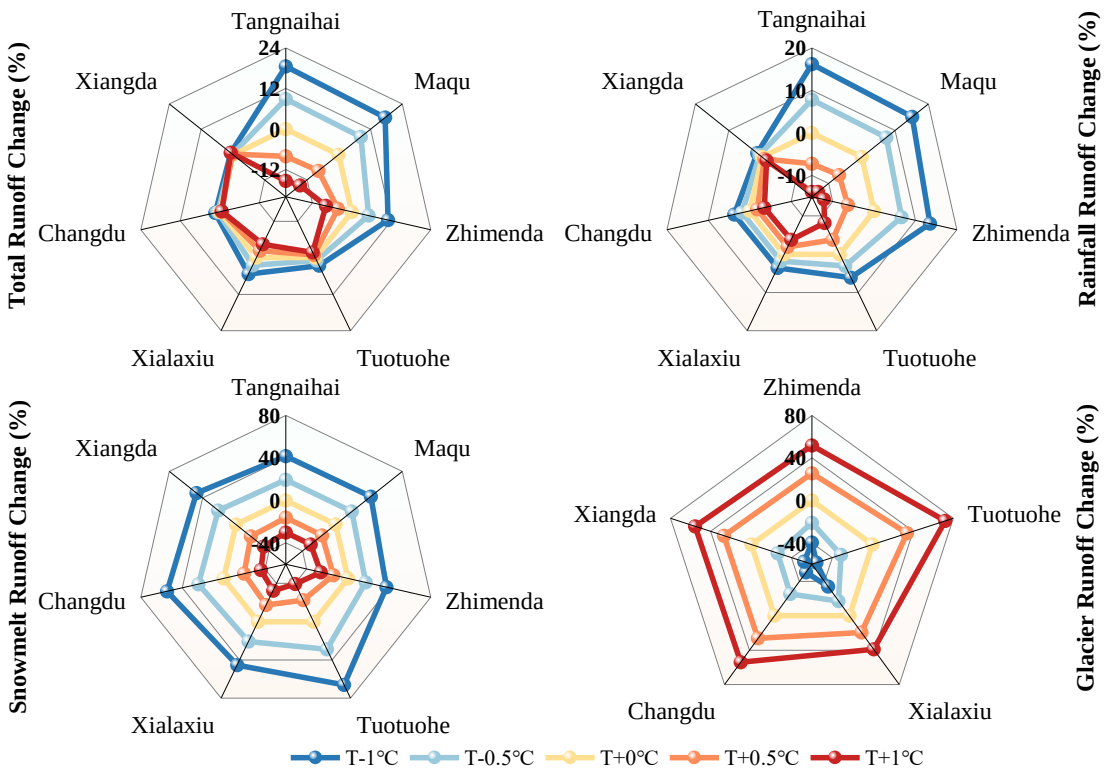

Figure S4. Percentage change in mean annual total, rainfall, snowmelt, and glacier runoff relative to the period 1984–2018 under temperature-change scenarios for the seven stations.

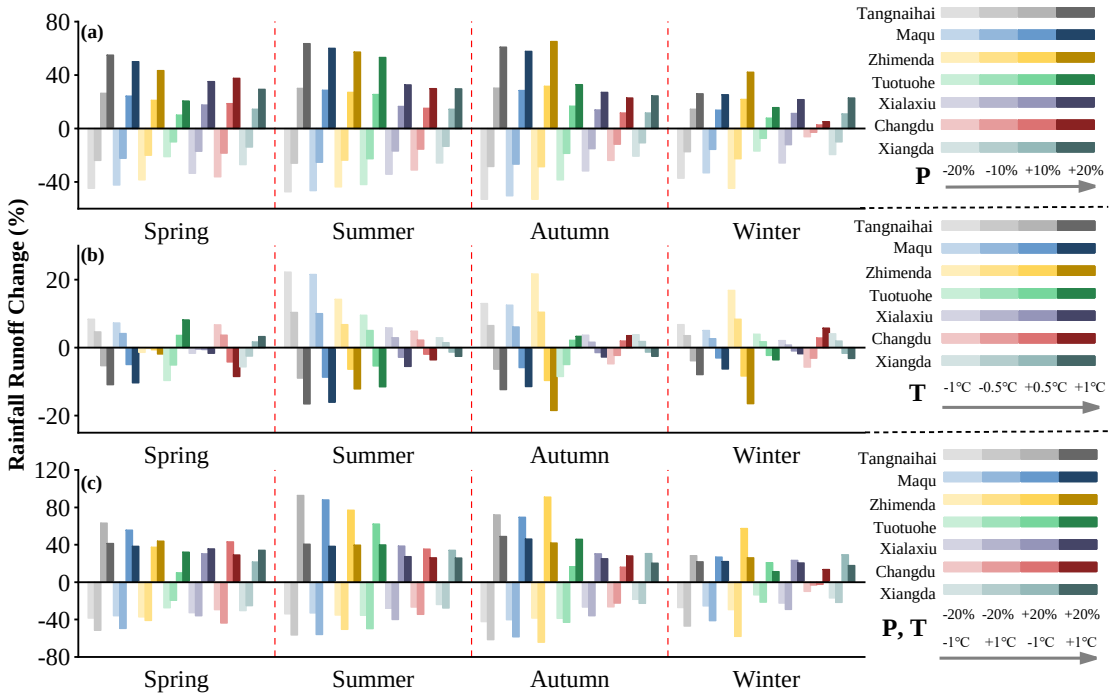

Figure S5. Seasonal percentage change in rainfall runoff relative to the period 1984–2018 under various scenarios for the seven stations. (a) Considering precipitation changes only; (b) Considering temperature changes only; (c) Considering precipitation and temperature changes simultaneously.

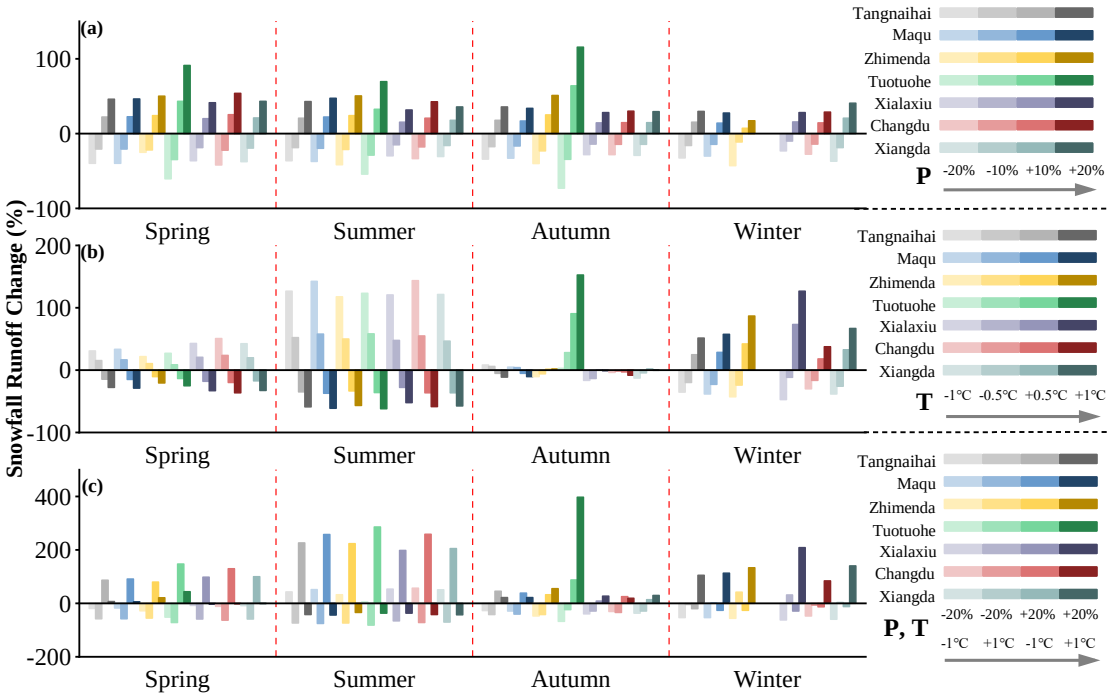

Figure S6. Seasonal percentage change in snowmelt runoff relative to the period 1984–2018 under various scenarios for the seven stations. (a) Considering precipitation changes only; (b) Considering temperature changes only; (c) Considering precipitation and temperature changes simultaneously.

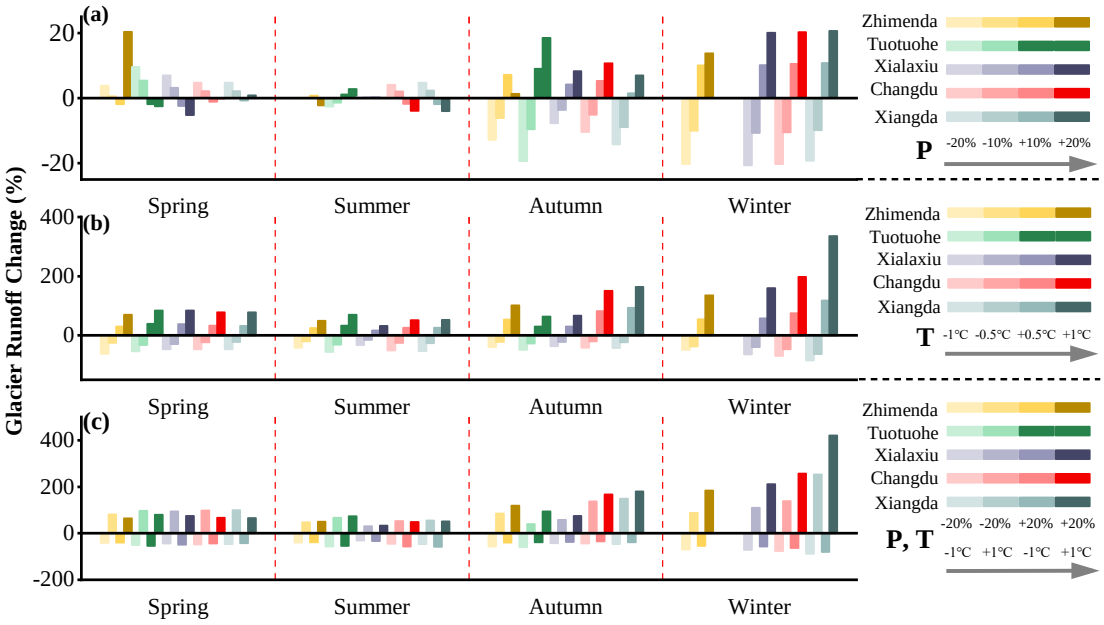

Figure S7. Seasonal percentage change in glacier runoff relative to the period 1984–2018 under various scenarios for the seven stations. (a) Considering precipitation changes only; (b) Considering temperature changes only; (c) Considering precipitation and temperature changes simultaneously.

References

Bennett, K. E., Blanco, J. R. U., Jonko, A., Bohn, T. J., Atchley, A. L., Urban, N. M., and Middleton, R. S.: Global Sensitivity of Simulated Water Balance Indicators Under Future Climate Change in the Colorado Basin, Water Resour. Res., 54, 132-149, https://doi.org/10.1002/2017wr020471, 2018.

Demaria, E. M., Nijssen, B., and Wagener, T.: Monte Carlo sensitivity analysis of land surface parameters using the Variable Infiltration Capacity model, J. Geophys. Res.-Atmos., 112, https://doi.org/10.1029/2006jd007534, 2007.

Shi, X., Wood, A. W., and Lettenmaier, D. P.: How Essential is Hydrologic Model Calibration to Seasonal Streamflow Forecasting?, J. Hydrometeorol., 9, 1350-1363, https://doi.org/10.1175/2008jhm1001.1, 2008.